

<https://africanjournalofbiomedicalresearch.com/index.php/AJBR>

Afr. J. Biomed. Res. Vol. 27(4s) (December 2024); 5778-5794

Research Article

Enhancement Method for Augmenting Blood Vessels of Retinal Images

Vandana^{1*}, Vijay Laxmi², Shalu Gupta³

¹*Research Scholar, vandanasingla3157@gmail.com, Dept. of Computer Science and Engineering, Guru Kashi University, Talwandi Sabo, Punjab, India

²Professor, drvijaylaxmi2003@gmail.com, Dept. of Computer Applications, Guru Kashi University, Talwandi Sabo, Punjab, India

³Assistant Professor, shalu2324@gmail.com, Dept. of Computer Applications, Guru Kashi University, Talwandi Sabo, Punjab, India

***Corresponding Author: Vandana**

*Research Scholar, vandanasingla3157@gmail.com, Dept. of Computer Science and Engineering, Guru Kashi University, Talwandi Sabo, Punjab, India

Abstract

Diabetes can cause changes in the blood vessels of the retina, causing them to swell and leak fluid. Diabetic Retinopathy (DR) is a common impediment of diabetes and is the primary cause of preventable blindness. Structural and functional alterations take place in different retinal cells comprising neurons, retinal endothelial cells, and retinal pigment epithelium before clinical symptoms of DR. The appearance of microaneurysms and diabetic macular edema leads to vision loss. The research paper focuses on enhancing the retinal images to detect the occurrence of early symptoms so that the treatment advances in an accurate direction. The research paper demonstrates the enhancement of retinal images obtained from the DRIVE dataset using CLAHE and Morphological methods. The proposed method made use of a Fisher Information matrix and Kalman filter for reducing noise and blurring regions of an image. The vesselness of the retinal images obtained from the DRIVE dataset has been conducted on five scales (0.3, 0.5, 1.0, 1.5, and 2.0) to extract the blood vessels from the retinal images.

The vesselness is conducted in both RGB and grayscale modes. The obtained ten vessel images (five colored and five grayscale) are compared with the original input image.

The colored vessel images are compared with the colored input image and the grayscale vessel images are compared with the grayscale input image. The vessel image with the highest value of PSNR and lowest value of MSE and RMSE is selected for further processing.

The proposed method makes use of a Histogram Equalization (HE), linear filter, and spatial filter for the removal of noise, and Gamma Transformation for enhancing the retinal images. The percentage of enhancement achieved by the proposed method as compared to CLAHE for MSE, RMSE, and PSNR are 98.23%, 86.81%, and 83.15% respectively, and against morphological operation is 94.93% for MSE, 77.67% for RMSE, and 41.68% for PSNR.

Keywords – CLAHE, Diabetic Retinopathy, DRIVE, PSNR.

***Author for correspondence: Email:**

Received: 01/12/2024

Accepted: 06/12/2024

DOI: <https://doi.org/10.53555/AJBR.v27i4S.4676>

© 2024 The Author(s).

This article has been published under the terms of Creative Commons Attribution-Noncommercial 4.0 International License (CC BY-NC 4.0), which permits noncommercial unrestricted use, distribution, and reproduction in any medium, provided that the following statement is provided. "This article has been published in the African Journal of Biomedical Research"

I. INTRODUCTION

People suffering from diabetes for an extended time and having poorly controlled blood sugar levels have a higher probability of suffering from Diabetic Retinopathy (DR). DR leads to loss of vision as the blood vessels of the retina undergo gradual destruction. The common symptoms of DR are having a dark spot in the middle of the eyesight, difficulty seeing at night, and blurred vision (Raman et al., 2022). DR is classified into two categories: Non-Proliferative Diabetic Retinopathy (NPDR) and Proliferative Diabetic Retinopathy (PDR). In NPDR, the symptoms are generally non-existent. Due to weakness, the small blood vessels leak blood. The leaked blood or fluid reaches the macula causing it to swell which results in blurred vision. PDR is a progressive stage of the disease. The retina is deprived of oxygen because of circulation impediments. This leads to the coming up of fragile blood vessels that grow in the retina and the back of the eye is filled with gel-like fluid (Rom et al., 2022). The newly formed blood vessels leak blood into the center of the eye resulting in blurred eyesight.

The research has been conducted using the retinal images from the Digital Retinal Images for Vessel Extraction (DRIVE) dataset. The DRIVE dataset has a total of 40 colored fundus images in .jpeg format which comprises 7 abnormal cases. The source of the images is the diabetic retinopathy screening program in the Netherlands. The Canon CR5 non-mydiatic 3CCD camera with a Field of View (FOV) equal to 45 degrees was used to capture the images. The resolution of each

image is 584*565 pixels with eight bits per color channel (Nagpal et al., 2022).

The research paper elaborates on the two most popular enhancement techniques used to enhance medical images, Contrast Limited Adaptive Histogram Equalization (CLAHE) and Morphological operations (MOs).

The four MOs (opening, dilation, erosion, and closing) have been analyzed and implemented on the retinal images. Section II discusses the conducted literature review. Section III elaborates on the three performance evaluation metrics: Mean Square Error (MSE), Root Mean Square Error (RMSE), and Peak Signal Noise Ratio (PSNR) with equations and examples. Section IV discusses the two existing enhancement techniques: CLAHE and MOs with their respective flowcharts. Section V elaborates on the proposed method designed and implemented for enhancing the retinal images with a detailed flowchart. Section VI illustrates the implementation of the proposed method. Section VII shows the obtained results followed by Section VIII discussing the conclusion.

II. LITERATURE REVIEW

The aim of conducting the literature survey is to gather relevant and timely research conducted on the topic chosen for research. The conducted survey needs to be blended into a cohesive summary of existing knowledge in the field. The section presents the conducted literature review in Table 1.

Table 1. Literature Review

References	Techniques	Methods / Models	Performance Evaluation parameters	Datasets	Findings / Results
Hayati et al., 2023	CLAHE, DL (Deep Learning), CNN (Convolutional Neural Network)	SGD (Stochastic Gradient Descent) optimizer	Average accuracy, Training Time, Epoch, Training accuracy, Train loss, Validation accuracy, Validation loss	APTOS 2019	Average Accuracy (original image): VGG16 [87%], InceptionV3 – [90%], Efficient Net – [95%], ResNet34 – [95%] And Average Accuracy (CLAHE): VGG16 [91%], InceptionV3 – [95%], Efficient Net – [97%], ResNet34 – [84%]
Malhi et al., 2023	GLCM (Gray Level Co-occurrence Matrix), Green Channel, CLAHE	SVM, KNN, DT, Top-hat filtering, Bottom-hat filtering	Contrast, Correlation, Energy, Homogeneity, Accuracy, Sensitivity, Specificity, ROC	Messidor, DiaretDb and E-oPhtha	DT tree performs well for grading via microaneurysms with an accuracy of 99.9% whereas SVM and KNN perform well for grading via exudates with an accuracy of 92.1%.

Wan et al., 2022	CLAHE, DL, CNN, GAN	Fusion-based, MSRCP, LIME, Cycle-GAN	BRISQUE (Blind/Referenceless image spatial quality evaluator), HUE	EyePACS, DRIVE, STARE, CHASEDB1, Proprietary dataset provided by the Affiliated Eye Hospital of Nanjing Medical University	Proposed DL-based method overcomes the shortcomings of traditional methods, such as color distortion and complex calculations
Mujeeb Rahman et al., 2022	SVM, DNN	ML, GLCM feature	Accuracy, Sensitivity, Specificity,	Public data repositories: Kaggle,	The SVM model had a mean AUC of 97.11%,
			Precision, F1-score, AUC	DDR, Zenodo, and Mendeley	whereas the DNN model had a mean AUC of 99.15%
Bataineh & Almotairi, 2021	Bilateral filters, uneven illumination correction method, HSV color model	HE, CS, CLAHE, Zhou's method	PSNR, MSE, SSIM, Entropy	DRIVE, STARE	The proposed method achieves the highest accuracy rate for contrast (C) and contrast improvement index (CII) measurements
Tsiknakis et al., 2021	DL (Deep Learning), AI (Artificial Intelligence)	CNN, Non-Local Means Denoising (NLMD), GAN (Generative Adversarial Networks)	Accuracy, Sensitivity, Specificity, F1- score, IoU, AUC, Cohen's Kappa	DiaretDB1 & e-Ophtha, IDRiD, Kaggle EyePACS	Explored DL in diagnosing DR
Hemanth et al., 2020	DL, HE, CLAHE	CNN	Accuracy, Sensitivity, Specificity, Precision, FScore, GMean	MESSIDOR	Accuracy - 97%, Sensitivity - 94%, Specificity - 98%, Precision - 94%, FScore - 94%, and GMean - 95%
Qureshi, Ma, & Shaheed, 2019	HE, AHE, CLAHE, and ESIHE	CIECAM02 color model	PSNR, CNR, Entropy, Histograms, SSIM	DRIVE, MESSIDOR	The proposed method outperformed the existing techniques as per the readings obtained for different performance metrics
Bandara et al., 2018	SUACE (Speeded up adaptive contrast enhancement)	Tyler Coye algorithm, Hough line transformation	TPR, FPR, Accuracy	STARE, DRIVE	The proposed work showed the superiority of SUACE in enhancing retinal images for blood vessel segmentation

Dai et al., 2016	HE, CLAHE, Normalized convolution with a domain transform	Green Channel, Two-stage denoising method, Fourth order PDEs, Median filter	CII (Contrast Improvement Index), Linear Index of Fuzziness, Average Running Time	DRIVE, STARE, DIARETDB1	The proposed method achieves a better performance on enhancing retinal fundus image comparing with the other methods
Shome & Vadali, 2011	SHE (Standard Histogram Equalization), CLAHE	Median filter	NPSD (Normalised Power Spectral Distribution), CPS (Cumulative Power Spectra)	DRIVE, Southern California College of Optometry	Intensity, Saturation, and noise amplification issues are addressed

III. PERFORMANCE EVALUATION METRICS

The performance evaluation parameters are the quantifiable and significant measure used for evaluating the performance of algorithms. The research work made use of three such parameters mentioned as

under.

A. MSE (Mean Square Error)

The MSE signifies the cumulative squared error between the compressed and the original image.

$$\frac{1}{n} \sum_{i=1}^n (Y_i - \hat{Y}_i)^2$$

Where

- * n is the number of data points
- * Y_i represents observed values
- * \hat{Y}_i represents predicted values

B. RMSE (Root Mean Square Error)

RMSE is a square root of MSE. It is used to calculate the variance between the source image and the segmented image. The lower the value of RMSE, the better the segmentation performance.

$$RMSE = [MSE]^{1/2}$$

C. PSNR (Peak Signal Noise Ratio)

PSNR is a universally used image processing function for comparing two images. PSNR is defined as a proportion between the determined power of an image and the power of noise hindering the quality of its representation. It is the most basic approximation of the difference between two images and is grounded on MSE. The PSNR is calculated by comparing the image with a perfectly clean image.

$$PSNR = 10 \log_{10}[(L-1)^2/MSE]$$

Where

L – Number of maximum intensity levels

MSE – Mean Square Error

The higher value of the PSNR between two images indicates the greater closeness of the two images. If the two images are exactly similar to each other, the PSNR in such a case is infinity. As PSNR is a logarithmic scale, even minor improvements are enough. PSNR is intended to monitor the removal of noise.

Consider an example to calculate MSE, RMSE, and PSNR. Let's have an original array of 1*4 say [3 4 15 10] and a reconstructed array [3 5 17 9] and assume that the maximum value for each element is 35. The MSE for the reconstructed array is the mean difference between the original and reconstructed arrays and is

calculated as

$$MSE = \Sigma[(3-3)^2 (4-5)^2 (15-17)^2 (10-9)^2]$$

$$MSE = \Sigma[0 \ 1 \ 4 \ 1] = 6/4 = 1.5$$

$$RMSE = [1.5]^{1/2} = 1.2247$$

$$PSNR = 10 * \log_{10} (35^2 / MSE) = 10[2 \log_{10} (35) - \log_{10} (1.5)] = 29.12044$$

IV. PRELIMINARIES

A. CLAHE

CLAHE divides the images into relative regions and implements Histogram Equalization to each partition. CLAHE evens out the distribution of used grey values and highlights the hidden features of the images. CLAHE is different from ordinary AHE because it tends to limit contrast. CLAHE implements a clipping limit for addressing the matter of noise amplification. CLAHE restricts the augmentation by clipping the histogram at a predefined value called CDF (Cumulative Distribution Function) [16]. CLAHE splits an input image into non-overlapping contextual areas referred to as blocks or tiles. The two parameters governing the image quality in CLAHE are BS (Block Size) and CL (Clip Limit). On increasing the CL, the brightness of the image increases as the image is of low intensity and the higher CL makes the histogram flatter. On increasing the BS, the contrast of the image increases with the expansion in the dynamic range. These two parameters at the point of maximum entropy curvature generate an image of good quality when using image entropy. Fig. 1 shows the approach adopted to apply CLAHE to enhance the retinal images. The retinal image from the DRIVE dataset is taken as input. The

spatia filter is applied to the input image to remove the noise from the image. After the removal of the noise, the highest and lowest pixel values of the image are obtained. The image is then converted to grayscale. Thereafter, padding is conducted on the image to create space around the content of elements within the

boundaries which allows for a more accurate analysis of the image [17]. The pixel count is computed for each contextual area and the values of performance evaluation metrics like PSNR, MSE, and RMSE are calculated between the input and enhanced image.

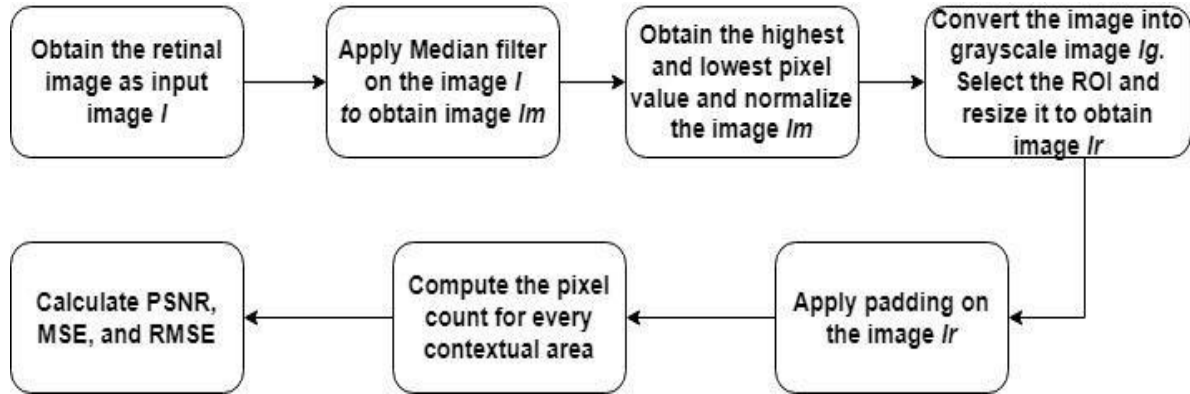


Fig. 1 Methodology for implementing CLAHE

B. Morphological Operations (MOs)

The basic components of the MOs are the image and the SE (Structuring Element). The SE is smaller than the image and slides over the image to alter it and generate an image of identical size. There are four different morphological operations mentioned below.

- Dilation – Dilation results in creating objects larger in size. It broadens the foreground pixels having a value of 1 and contracts the background pixels having a value of 0. The pixel having a value of 1 in the neighboring is set to 1.
- Erosion – Erosion results in creating objects smaller in size. It broadens the background pixels having a value of 0 and contracts the foreground pixels having a value of 1. The pixel having a value of 0 in the neighboring is set to 0.

- Opening – In the opening, the image is first eroded followed by dilation. Opening preserves the shape and size of the larger objects eradicating the smaller objects from the image.
 - Closing – In closing, the image is first dilated followed by erosion. Closing preserves the shape and size of the objects and fills the small holes in the image.
- Fig. 2 depicts the methodology obtained for implementing the MOs on the retinal images of the DRIVE dataset. Consider an input image and convert it to grayscale. Perform the four MOs on the image to obtain four output images. Compare each output image with the input image and calculate the performance evaluation metrics. Look for the case with the highest PSNR and lowest MSE and RMSE to find the best among the four operations.

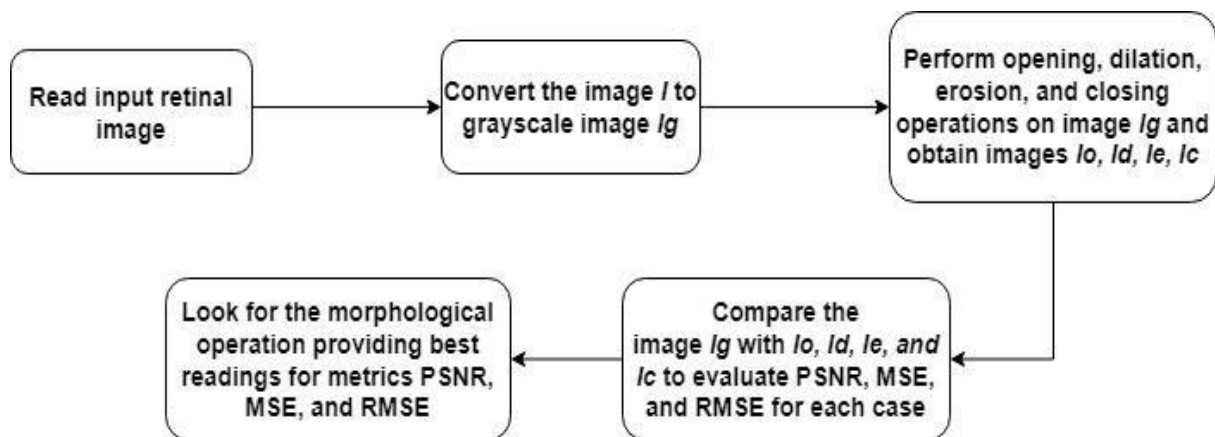


Fig. 2 Methodology for implementing Mos

V. CONTRIBUTION

Fig. 3 shows the proposed method for enhancing the retinal images. The proposed method made use of a FisherInformation matrix and Kalman filter. The Fisher information is a method of determining the amount of information that a noticeable random variable X transfers about an unidentified parameter θ upon which the probability of X depends. Kalman filter

uses a sequence of measurements perceived over time comprising statistical noise and other inconsistencies to generate approximations of unknown variables that incline to be more precise than those grounded on a single measurement alone by approximating a joint probability distribution over the variables for each timeframe. The vesselness of the retinal images obtained from the DRIVE dataset has been conducted

on five scales (0.3, 0.5, 1.0, 1.5, and 2.0) to extract the blood vessels from the retinal images. The vesselness is steered in both RGB and grayscale modes. The ten obtained vesseled images (five colored and five grayscale) are compared with the original input image. The colored vesseled images are compared with the colored input image and the grayscale vesseled images are compared with the grayscale input image. The vesseled image with the highest value of PSNR and lowest value of MSE and RMSE is selected for further processing. The proposed method makes use of a

Histogram Equalization (HE), linear filter, and spatial filter for introducing blurring intended to remove the small details from the image followed by noise reduction, and Gamma Transformation for enhancing the retinal images. The enhancement of the images differs from the variation in the value of γ (gamma). Each display device has its gamma correction which results in displaying the images at different intensities. Fig. 3 shows the detailed flowchart illustrating the research methodology adopted for enhancing the retinal images using the proposed method.

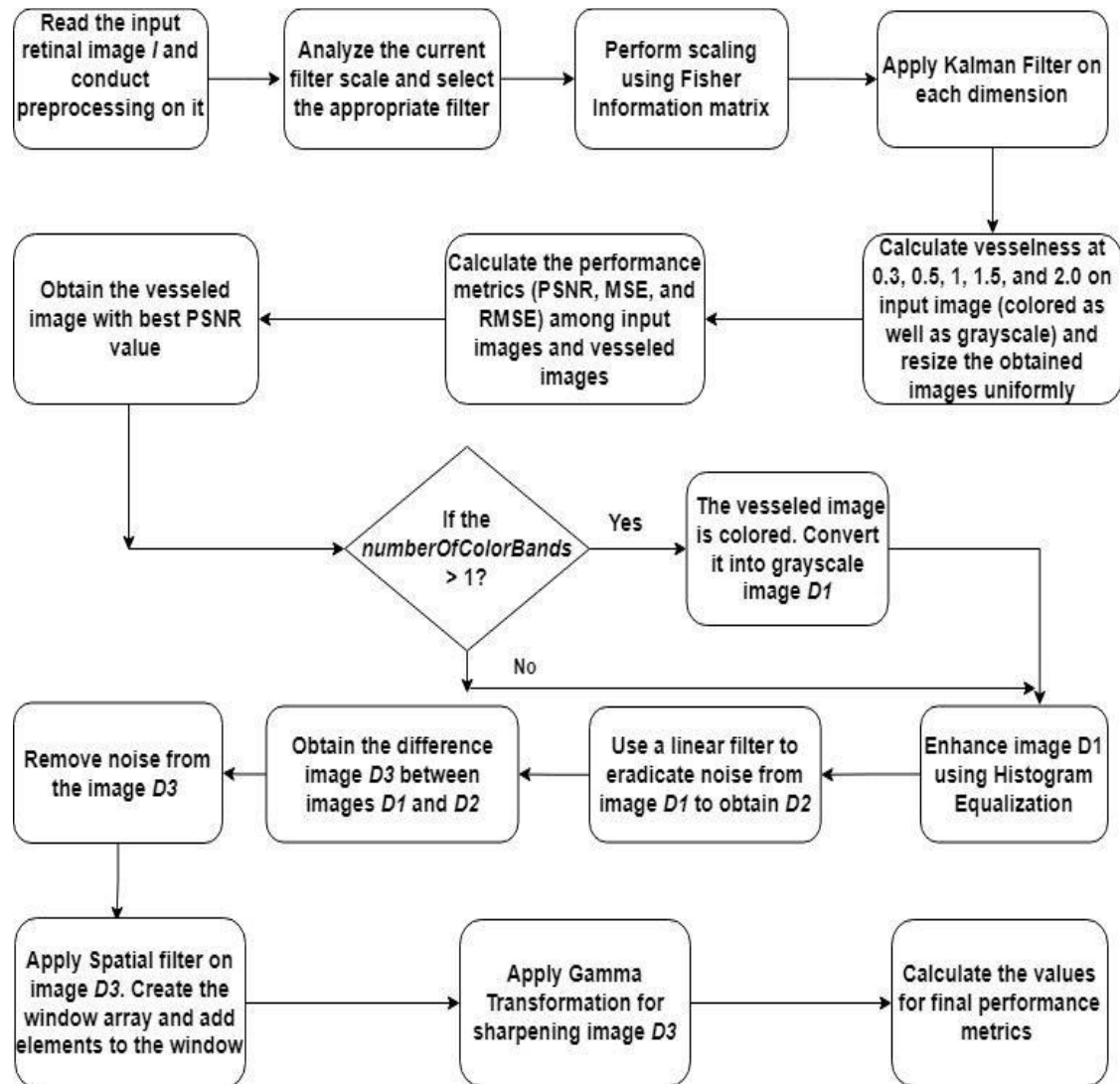


Fig. 3 Proposed method

Vesselness scales	Image type	MSE	RMSE	PSNR
0.3	Colored	7.4671	2.7326	30.67
0.5	Colored	9.2789	3.0461	28.78
1.0	Colored	11.9294	3.4539	26.60
1.5	Colored	12.8855	3.5896	25.93
2.0	Colored	9.2789	3.0461	28.78

VI. IMPLEMENTATION

This section focuses on the implementation of the proposed method on image 34_training.tif from the DRIVE dataset.

Fig. 4 shows the images obtained after applying vesselness at five levels (0.3, 0.5, 1.0, 1.5, and 2.0).

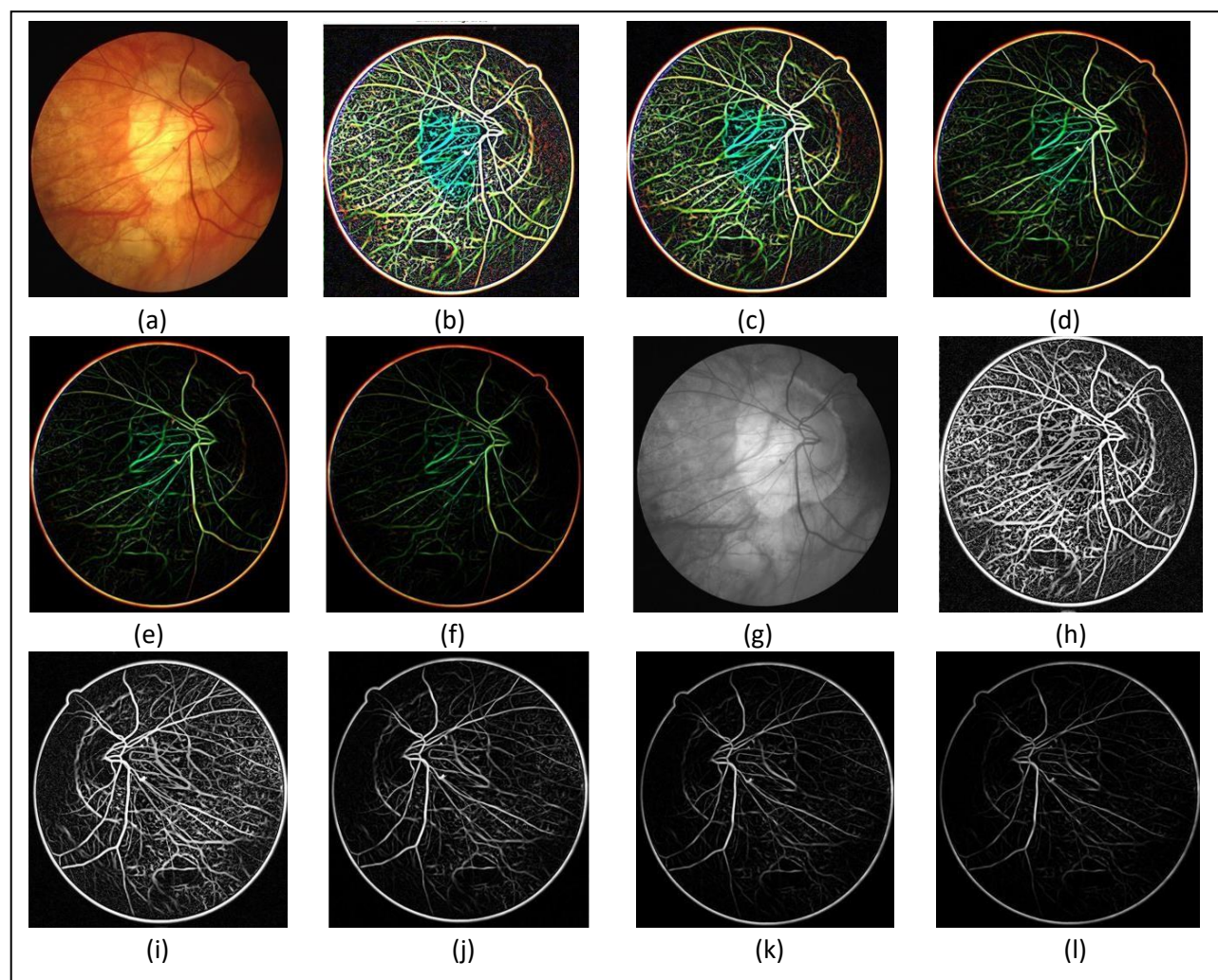


Fig. 4 (a) Colored Input image (b) Colored vesseled image at 0.3 (c) Colored vesseled image at 0.5 (d) Colored vesseled image at 1.0 (e) Colored vesseled image at 1.5 (f) Colored vesseled image at 2.0 (g) Grayscale input image (h) Grayscale vesseled image at 0.3 (i) Grayscale vesseled image at 0.5 (j) Grayscale vesseled image at 1.0 (k) Grayscale vesseled image at 1.5 (l) Grayscale vesseled image at 2.0

Table 2 shows the reading of performance evaluation metrics obtained after comparing the five different scales of vesselness with the input image. The colored input image is compared with the colored vesseled images and the grayscale input image is compared with the grayscale vesseled image.

0.3	Grayscale	10.2991	3.2092	27.87
0.5	Grayscale	11.9272	3.4536	26.60
1.0	Grayscale	4.1119	2.0278	35.85
1.5	Grayscale	13.5314	3.6785	25.50
2	Grayscale	13.6240	3.6911	25.44

The best results have been obtained for vesselness conducted at scale 1 for grayscale images with PSNR of highest PSNR of 35.85 dB and lowest values of MSE of 4.1119 and RMSE of 2.0278 respectively.

The vesseled grayscale image at scale 1.0 is provided as input to the proposed model. Firstly, the vesseled image is normalized to obtain image $D1$ as shown in Fig. 5(a)

followed by the removal of noise from the retinal image using a Kalman filter as in Fig. 5(b). The image is enhanced using the adaptive filter to obtain image $D2$ as in Fig. 5(c). Thereafter the difference image is obtained after subtracting $D1$ from $D2$ as in Fig. 5(d). Finally, the Gamma Transformation is applied to the different images to obtain the image in Fig. 5(e).

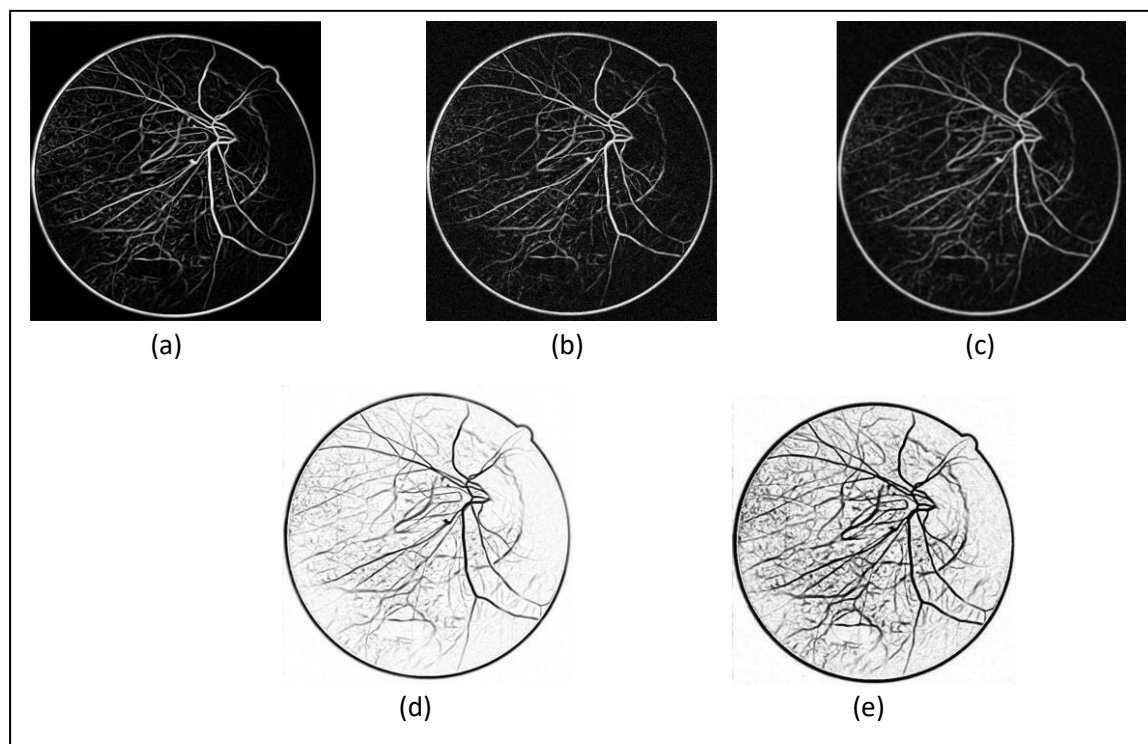


Fig. 5 (a) Normalized vesseled image $D1$ (b) Removal of noise using Kalman filter (c) Enhanced image after applying filters $D2$ (d) Difference image ($D1 - D2$) (e) Gamma Transformation applied on the difference image.

The readings of the three performance metrics obtained after applying the proposed method are mentioned below.

$MSE - 0.3035$




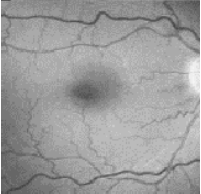

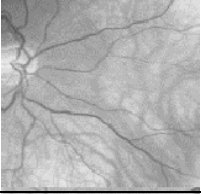
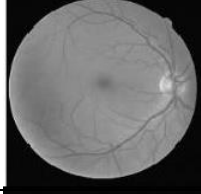
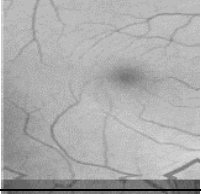


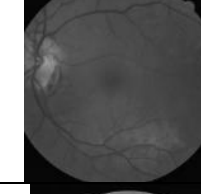
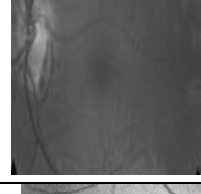

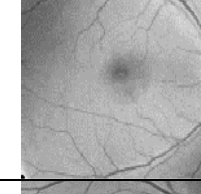
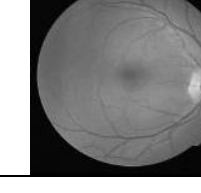
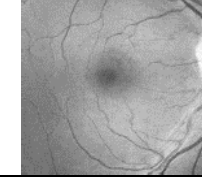
$RMSE - 0.5509$

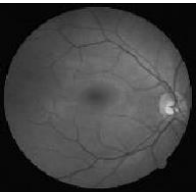


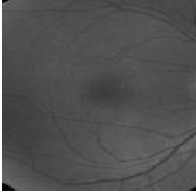
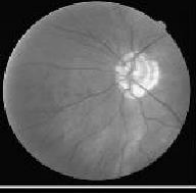


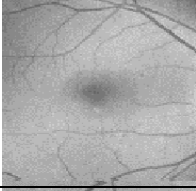
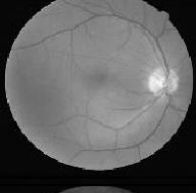
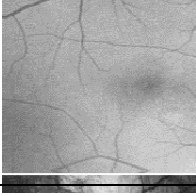
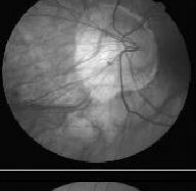
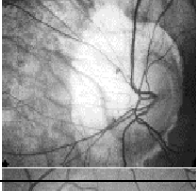
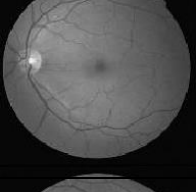
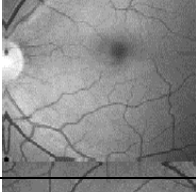
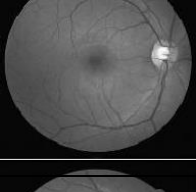
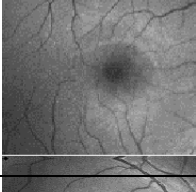


$PSNR - 58.49 \text{ dB}$

DRIVE dataset. Table 3 shows the MSE, RMSE, and PSNR values for 20 retinal pictures from the DRIVE dataset.

VII. RESULTS

This section elaborates on the results obtained for each of the three approaches used to enhance the retinal images in the

Image name	Input Image	MSE	RMSE	PSNR (dB)	Output image
21_training.pgm		6.3487	2.5197	32.08	
22_training.pgm		6.3649	2.5229	32.05	
23_training.pgm		6.3010	2.5102	32.14	
24_training.pgm		6.1486	2.4796	32.36	
25_training.pgm		7.5986	2.7566	30.52	
26_training.pgm		8.3806	2.8949	29.67	
27_training.pgm		6.2659	2.5032	32.19	
28_training.pgm		6.4131	2.5324	31.99	

29_training.pgm		7.9348	2.8169	30.14	
30_training.pgm		8.3125	2.8831	29.74	
31_training.pgm		5.2645	2.2945	33.70	
32_training.pgm		6.3762	2.5251	32.04	
33_training.pgm		6.3432	2.5186	32.08	
34_training.pgm		7.5347	2.7449	30.59	
35_training.pgm		7.2688	2.6961	30.90	
36_training.pgm		7.3629	2.7135	30.79	
37_training.pgm		6.8943	2.6257	31.36	

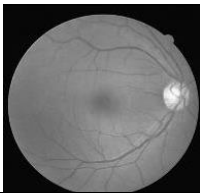
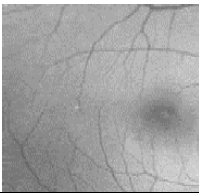

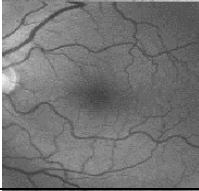

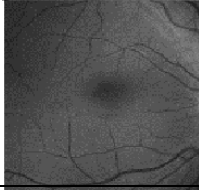
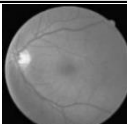
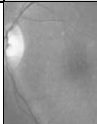
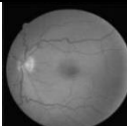

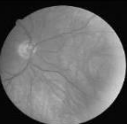
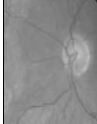


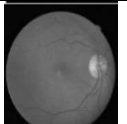
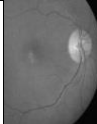
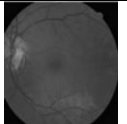
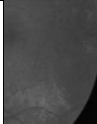
38_training.pgm			6.5418	2.5577	31.82	
39_training.pgm			7.8791	2.8070	30.20	
40_training.pgm			8.1758	2.8593	29.88	

Table 4 illustrates the performance data acquired for four MOs. The MSE, RMSE, and PSNR values are determined for 20 retinal images from the DRIVE dataset for each MO, and it is discovered that dilation outperformed the other three operations on all 20 images. As a result, among the four MOs, dilation operation readings are the most precisely recorded.

Image name (*.pgm)	Input image	Opening			Dilated			Eroded			Closing			Output image
		MSE	RMSE	PSNR	MSE	RMSE	PSNR	MSE	RMSE	PSNR	MSE	RMSE	PSNR	
21_training		5.5312	2.3519	33.27	2.6746	1.6354	39.59	5.3291	2.3085	33.60	5.5312	2.3519	33.27	
22_training		4.8145	2.1942	34.48	2.5603	1.6001	39.96	4.6549	2.1575	34.77	4.8145	2.1942	34.48	
23_training		5.2379	2.2886	33.75	2.6966	1.6421	39.51	5.0351	2.2439	34.09	5.2379	2.2886	33.75	
24_training		4.5606	2.1356	34.95	2.3661	1.5382	40.65	4.4275	2.1042	35.21	4.5606	2.1356	34.95	
25_training		4.5537	2.1339	34.96	1.8797	1.3710	42.65	4.2128	2.0525	35.64	4.5537	2.1339	34.96	
26_training		4.1101	2.0273	35.85	1.9304	1.3894	42.42	3.8655	1.9661	36.39	4.1101	2.0273	35.85	



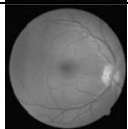
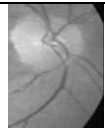
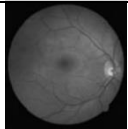
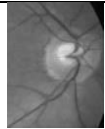
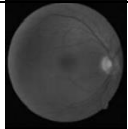
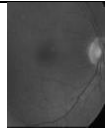
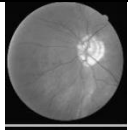
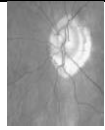

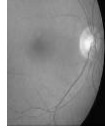
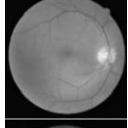
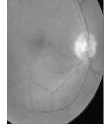
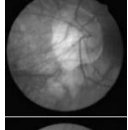
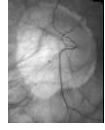
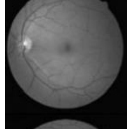
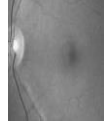
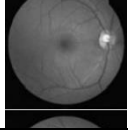
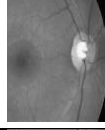
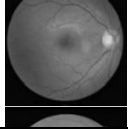
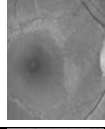
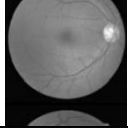
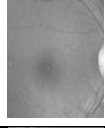
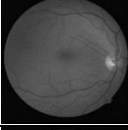
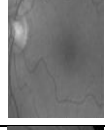

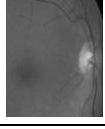
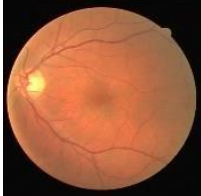
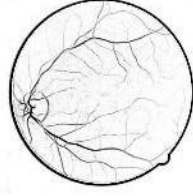
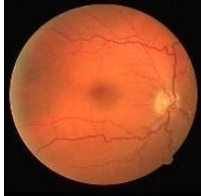
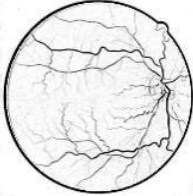

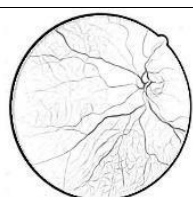

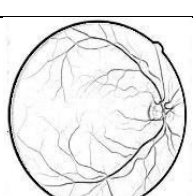

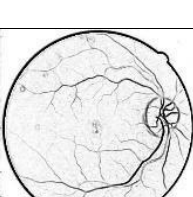

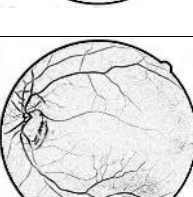

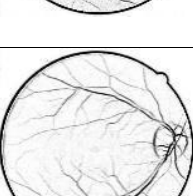

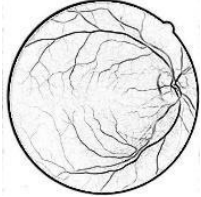

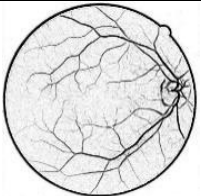

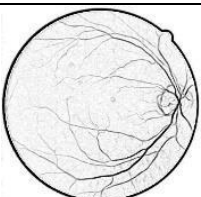

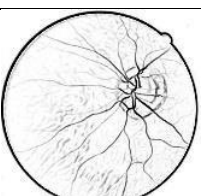
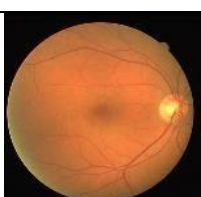
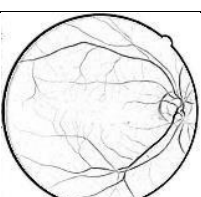
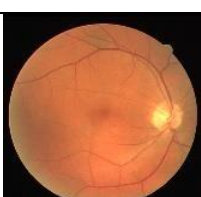
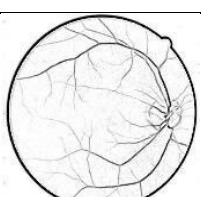

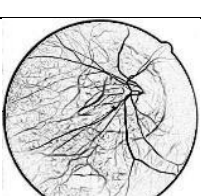

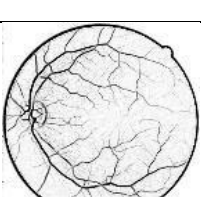

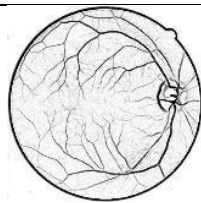

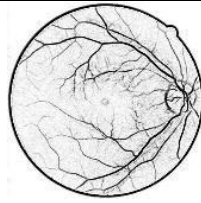

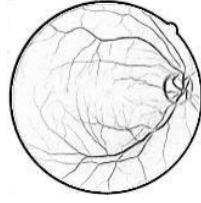

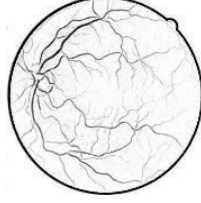

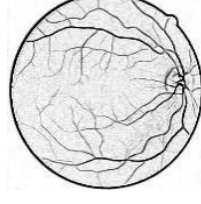
27_training		4.8 190	2.1 952	34. 47	2.6 690	1.6 337	39. 60	4.6 740	2.1 619	34. 74	4.8 190	2.1 952	34. 47	
28_training		7.7 437	2.7 827	30. 35	3.0 767	1.7 541	38. 37	7.2 096	2.6 851	30. 97	7.7 437	2.7 827	30. 35	
29_training		6.9 335	2.6 332	31. 31	2.9 531	1.7 185	38. 73	6.4 851	2.5 466	31. 89	6.9 335	2.6 332	31. 31	
30_training		3.9 669	1.9 917	36. 16	2.1 169	1.4 550	41. 62	3.8 538	1.9 631	36. 41	3.9 669	1.9 917	36. 16	
31_training		6.1 602	2.4 820	32. 34	2.4 681	1.5 710	40. 28	5.9 456	2.4 384	32. 65	6.1 602	2.4 820	32. 34	
32_training		4.8 288	2.1 975	34. 45	1.8 897	1.3 747	42. 60	4.5 125	2.1 243	35. 04	4.8 288	2.1 975	34. 45	
33_training		5.2 850	2.2 989	33. 67	1.9 390	1.3 925	42. 38	5.1 150	2.2 616	33. 95	5.2 850	2.2 989	33. 67	
34_training		7.0 257	2.6 506	31. 20	2.3 106	1.5 201	40. 86	6.7 449	2.5 971	31. 55	7.0 257	2.6 506	31. 20	
35_training		5.5 577	2.3 575	33. 23	2.6 051	1.6 140	39. 81	5.4 015	2.3 241	33. 48	5.5 577	2.3 575	33. 23	
36_training		5.6 640	2.3 799	33. 07	2.2 457	1.4 986	41. 10	5.4 505	2.3 346	33. 40	5.6 640	2.3 799	33. 07	
37_training		6.4 337	2.5 365	31. 96	2.7 967	1.6 723	39. 20	6.3 551	2.5 209	32. 07	6.4 337	2.5 365	31. 96	
38_training		5.1 724	2.2 743	33. 86	2.5 262	1.5 894	40. 08	5.1 007	2.2 585	33. 98	5.1 724	2.2 743	33. 86	
39_training		4.8 163	2.1 946	34. 48	2.6 543	1.6 292	39. 65	4.6 754	2.1 635	34. 73	4.8 163	2.1 946	34. 48	
40_training		4.9 438	2.2 235	34. 25	2.4 116	1.5 529	40. 48	4.7 908	2.1 888	34. 52	4.9 438	2.2 235	34. 25	

Table 5: displays the results of the performance metrics acquired for the proposed technique. MSE, RMSE, and PSNR values were calculated for 20 retinal images from the DRIVE dataset, and it was discovered that for all 20 images, the readings of all performance metrics are higher than the readings obtained in Table 3 for CLAHE and Table 4 for MOs. The proposed technique outperformed both CLAHE and MOs in improving retinal images.

Image name	Input Image	MSE	RMSE	PSNR(dB)	Output image
21_training.tif		0.1347	0.3670	56.83	
22_training.tif		0.1075	0.3279	57.81	
23_training.tif		0.1032	0.3212	57.99	
24_training.tif		0.1107	0.3327	57.69	
25_training.tif		0.1063	0.3260	57.86	
26_training.tif		0.1361	0.3689	56.79	
27_training.tif		0.0964	0.3104	58.29	

28_training.tif		0.1534	0.3917	56.27	
29_training.tif		0.1241	0.3523	57.19	
30_training.tif		0.1097	0.3312	57.73	
31_training.tif		0.0875	0.2958	58.71	
32_training.tif		0.1589	0.3986	56.11	
33_training.tif		0.1364	0.3693	56.78	
34_training.tif		0.0563	0.2373	60.62	
35_training.tif		0.1544	0.3929	56.24	

36_training.tif		0.1489	0.3858	56.40	
37_training.tif		0.1636	0.4045	55.99	
38_training.tif		0.0834	0.2888	58.92	
39_training.tif		0.1324	0.3639	56.91	
40_training.tif		0.1658	0.4071	55.93	

VIII. CONCLUSION

The higher the PSNR number and the lower the MSE and RMSE values, the greater the degree of improvement accomplished. The average MSE and RMSE for CLAHE are 6.9855 and 2.6430, respectively, which are the highest. The proposed technique achieves the lowest MSE and RMSE values (0.1235 and 0.3487, respectively). The dilation operation achieves the lowest MSE and RMSE among the MOs, at 2.43852 and

1.5616, respectively. The proposed technique achieved the maximum PSNR of 57.35 dB, outperforming the CLAHE and MOs. The CLAHE has the lowest average PSNR (31.312). The best average PSNR for dilation operations is 40.477 dB, while the lowest average PSNR for opening and closure operations is 33.603. The results in Table 6 show that the suggested method outperformed existing ways of improving retinal images in all operations.

Table 6. Comparative mean values of performance metrics for CLAHE, MOs, and proposed method

Average MSE		Average RMSE	Average PSNR
CLAHE	6.9855	2.6430	31.312
Opening (MO)	5.4079	2.3254	33.603
Dilation (MO)	2.4385	1.5616	40.477
Erosion (MO)	5.1919	2.2785	33.95
Closing (MO)	5.4079	2.3255	33.603
Proposed Method	0.1235	0.3487	57.35

Fig. 6, 7, and 8 show the graphical representation of average MSE, average RMSE, and average PSNR respectively. The proposed method has the lowest average MSE **and RMSE and the highest value of average PSNR.**

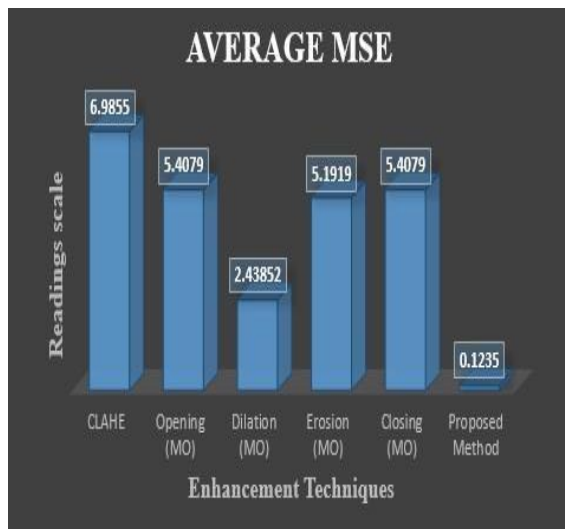


Fig. 6 Average MSE

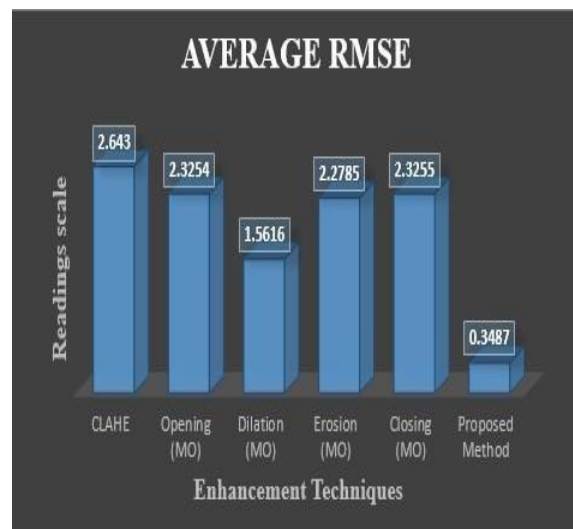


Fig. 7 Average RMSE

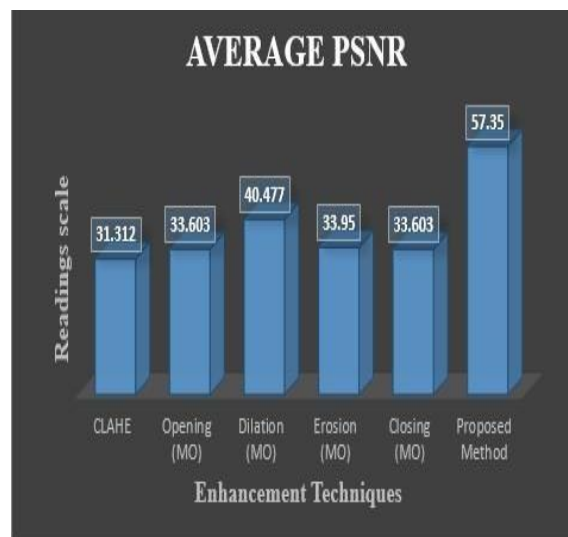


Fig. 8 Average PSNR

The percentage of enhancement achieved by the proposed method as compared to CLAHE and MO (dilation) is shown in Table 7. As dilation provided the

best results for the performance evaluation metrics as shown in Table6, so in MOs only dilation is compared with the proposed method.

Table 7. Percentage of enhancement achieved

Enhancement percentage	MSE	RMSE	PSNR
CLAHE and Proposed method	98.23%	86.81%	83.16%
MO (dilation) and Proposed method	94.93%	77.67%	41.68%

REFERENCES

- Bandara, A. M. R. R., Rajarata, K. A. S. H. K., & Giragama, P. W. G. R. M. P. B. (2018). Super-efficient spatially adaptive contrast enhancement algorithm for superficial vein imaging. *2017 IEEE International Conference on Industrial and Information Systems, ICIIS 2017 - Proceedings, 2018-January*, 1–6. <https://doi.org/10.1109/ICIINFS.2017.8300427>
- Bataineh, B., & Almotairi, K. H. (2021). Enhancement Method for Color Retinal Fundus Images Based on Structural Details and Illumination Improvements. *Arabian Journal for Science and Engineering*, 46(9), 8121–8135. <https://doi.org/10.1007/s13369-021-05429-6>
- Bidwai, P., Gite, S., Pahuja, K., & Kotecha, K.

- (2022). A Systematic Literature Review on Diabetic Retinopathy Using an Artificial Intelligence Approach. *Big Data and Cognitive Computing*, 6(4). <https://doi.org/10.3390/bdcc6040152>
4. Dai, P., Sheng, H., Zhang, J., Li, L., Wu, J., & Fan, M. (2016). Retinal Fundus Image Enhancement Using the Normalized Convolution and Noise Removing. *International Journal of Biomedical Imaging*, 2016. <https://doi.org/10.1155/2016/5075612>
5. Hayati, M., Muchtar, K., Roslidar, Maulina, N., Syamsuddin, I., Elwirehardja, G. N., & Pardamean, B. (2023). Impact of CLAHE-based image enhancement for diabetic retinopathy classification through deep learning. *Procedia Computer Science*, 216(2022), 57–66. <https://doi.org/10.1016/j.procs.2022.12.111>
6. Hemanth, D. J., Deperlioglu, O., & Kose, U. (2020). An enhanced diabetic retinopathy detection and classification approach using deep convolutional neural network. *Neural Computing and Applications*, 32(3), 707–721. <https://doi.org/10.1007/s00521-018-03974-0>
7. Malhi, A., Grewal, R., & Pannu, H. S. (2023). Detection and diabetic retinopathy grading using digital retinal images. In *International Journal of Intelligent Robotics and Applications* (Issue 0123456789). Springer Nature Singapore. <https://doi.org/10.1007/s41315-022-00269-5>
8. Nagpal, D., Panda, S. N., Malarvel, M., Pattanaik, P. A., & Zubair Khan, M. (2022). A review of diabetic retinopathy: Datasets, approaches, evaluation metrics and future trends. *Journal of King Saud University - Computer and Information Sciences*, 34(9), 7138–7152. <https://doi.org/10.1016/j.jksuci.2021.06.006>
9. Qureshi, I., Ma, J., & Abbas, Q. (2019). Recent development on detection methods for the diagnosis of diabeticretinopathy. In *Symmetry* (Vol. 11, Issue 6). MDPI AG. <https://doi.org/10.3390/sym11060749>
10. Qureshi, I., Ma, J., & Shaheed, K. (2019). A Hybrid Proposed Fundus Image Enhancement Framework for Diabetic Retinopathy. *Algorithms*, 12(1). <https://doi.org/10.3390/a12010014>
11. Raman, R., Vasconcelos, J. C., Rajalakshmi, R., Prevost, A. T., Ramasamy, K., Mohan, V., Mohan, D., Rani, P.K., Conroy, D., Das, T., & Sivaprasad, S. (2022). Prevalence of diabetic retinopathy in India stratified by known and undiagnosed diabetes, urban-rural locations, and socioeconomic indices: results from the SMART India population-based cross-sectional screening study. *The Lancet. Global Health*, 10(12), e1764–e1773. [https://doi.org/10.1016/S2214-109X\(22\)00411-9](https://doi.org/10.1016/S2214-109X(22)00411-9)
12. Rom, Y., Aviv, R., Ianchulev, T., & Dvey-Aharon, Z. (2022). Predicting the future development of diabetic retinopathy using a deep learning algorithm for the analysis of non-invasive retinal imaging. *BMJ Open Ophthalmology*, 7(1), e001140. <https://doi.org/10.1136/bmjophth-2022-001140>
13. Shome, S., & Vadali, S. (2011). Enhancement of diabetic retinopathy imagery using contrast limited adaptivehistogram equalization. *International Journal of Computer Science and Information Technologies*, 2(6),2694–2699.
14. Tsiknakis, N., Theodoropoulos, D., Manikis, G., Ktistakis, E., Boutsora, O., Berto, A., Scarpa, F., Scarpa, A., Fotiadis, D. I., & Marias, K. (2021). Deep learning for diabetic retinopathy detection and classification based on fundus images: A review. *Computers in Biology and Medicine*, 135(June), 104599. <https://doi.org/10.1016/j.compbimed.2021.104599>
15. Wan, C., Zhou, X., You, Q., Sun, J., Shen, J., Zhu, S., Jiang, Q., & Yang, W. (2022). Retinal Image Enhancement Using Cycle-Constraint Adversarial Network. *Frontiers in Medicine*, 8(January), 1–16. <https://doi.org/10.3389/fmed.2021.793726>
16. T. E. Belay and S. Gupta (2024), Literature review Strategic Investigation of Open-SourceWeb Application Vulnerability Testing Tools: A Holistic Examination and Comparative Study, in Dandao Xuebao/Journal of Ballistics, ISSN: 1004-499X, Vol. 36, No. 1, pp. 91-101. <https://ballisticsjournal.com/index.php/journal/article/view/150/140>
17. T. E. Belay and S. Gupta (2024), Scientific Research Methodology for Strategic Investigation of Open-SourceWeb Application Vulnerability Testing Tools: A Holistic Examination and Comparative Study, in Journal of Electrical Systems, ISSN: 6946-6962. <https://journal.esrgroups.org/jes/article/view/6785/4702>